XMM-Newton Calibration Technical Note

XMM-SOC-CAL-TN-0096

The stability of the EPIC-pn camera

Matteo Guainazzi, Martin Stuhlinger, Nathan Dickinson, Andrew Pollock
(*ESA-ESAC, Villafranca del Castillo, Spain*)

November 23, 2012

History

Version	Date	Editor	Note
1.0	November 23, 2012	M.Guainazzi	First public version

1 Scope

In this report we investigate the stability of the EPIC-pn camera on board XMM-Newton (Strüder et al., 2001). "Stability" as measured in this document reflects all and each of optics plus detector system elements, and their calibration: effective area, filter transmission, quantum efficiency, and redistribution. This document discusses on-axis (within ≃15") observations only.

2 RXJ1856-3754

RXJ1856.6-3754 is one of the seven known isolated neutron stars (INSs) identified in the ROSAT All Sky Survey (Treves et al. 2000). Their X-ray spectrum is extremely soft, and can be generally well modelled by a blackbody with temperatures kT≃50-100 eV (Burwitz et al. 2003, 2001; Trümper et al. 2004), although one might expect deviations from a simple blackbody shape due to atmospheres of either heavy elements (due to debris from the progenitor) or light elements (gravitational setting or accretion; Ho et al. 2007). Interestingly enough, RXJ1856.6-3754 lacks broad spectral atmospheric features seen in other INSs such as RXJ0720.4-3125 (Haberl et al. 2004; Kaplan & van Kerkwijk 2005; Hambaryan et al. 2009).

Starting from 2004, RXJ1856-3754 has been observed approximately twice per year in the framework of the XMM-Newton Routine Calibration Plan (Guainazzi 2012). Tab. 1 reports the list of

Table 1: EPIC-pn configuration for the observations discussed in this document

Obs.#	Date (YYYY-MM-DDTHH:MM:SS)	RAWX	RAWY	T_{exp} (ks)	ΔPHA
0106260101	2002-04-08T16:21:27	38	191	39	1
0165971601	2004-09-24T01:42:13	38	190	22	-1
0165971901	2005-03-23T08:34:42	37	191	16	-1
0165972001	2005-09-24T07:58:13	38	191	22	2
0165972101	2006-03-26T15:40:29	37	191	48	4
0412600101	2006-10-24T00:33:51	38	190	50	3
0412600201	2007-03-14T20:50:01	38	191	21	-3
0415180101	2007-03-25T05:36:47	36	168	17	1
0412600301	2007-10-04T05:48:49	38	190	14	-1
0412600401	2008-03-13T18:49:45	37	191	33	3
0412600601	2008-10-05T01:00:58	39	190	43	0
0412600701	2009-03-19T21:30:04	36	191	47	4
0412600801	2009-10-07T15:20:44	38	190	38	1
0412600901	2010-03-22T02:50:25	37	191	50	3
0412601101	2010-09-28T23:09:10	36	192	47	4
0412601301	2011-03-14T00:47:48	37	179	48	1
0412601401	2012-04-13T07:12:25	36	179	31	3
0412602301	2012-09-20T11:23:08	40	189	50	0

observations discussed in this document together with their instrumental configuration. All observations discussed in this document were taken in *Small Window* (SW) with the `Thin` optical blocking filter.

2.1 Work published on the EPIC-pn stability, and our approach

Sartore et al.(2012) discuss the stability of the EPIC-pn camera using the same source (and most of the data) used in this document. Employing standard spectral fitting techniques, they conclude that no evidence of spectral or flux variations is detected from March 2005 to October 2011, once observations taken at the same detector position are considered. The 3σ upper limit on the 0.15-1.2 keV flux variation is 3%.

In this document, we present the result of a study aiming at the same goal. We follow a complementary approach based on the temporal evolution of background-subtracted count rates, to avoid astrophysical uncertainties in the conversion between instrumental counts and fluxes. Moreover, we apply a self-calibration of the energy reconstruction in PHA space (see Sect. 4, which allows us to make use of all on-axis data, notwithstanding the source position in detector coordinates .

3 Spectral fitting

In this Section we present for completeness the results of a standard spectral fitting. Data reduction followed the procedure described in Stuhlinger et al. (2011). Spectra were extracted from 37.5" radius circular regions around the X-ray source centroid. Background spectra were extracted from source-free boxes at the edge of the SW reading area. The spectrum of each camera and observation was fit in the 0.15-0.80 keV[1] energy band with a model constituted by a single blackbody component seen through a screen of neutral photoelectric absorption (in compact XSPEC jargon: `tbabs*bbody`), with all the parameters free to vary. While more complex models could be astrophysically justified (Burwitz et al. 2003), no consensus currently exists on *the* correct astrophysical model for RXJ1856-3754. Fig. 1 shows spectra and residuals against the best-fit model for all observations in Tab. 1. Readers are referred to Sartore et al. (2012) for a discussion of the spectral analysis results.

4 Count rate stability

Small column-by-column variations of the instrumental gain can substantially affect the measured count rates. Simulations indicate that a shift of ± 5 eV translates into a $\pm 5\%$ systematic error on the background subtracted count rate in the 0.15-0.8 keV band.

In order to minimise this effect, we applied a relative calibration method to all the RXJ1856.6-3754 spectra discussed in this document. We have chosen the spectrum with the longest expo-

[1] We intentionally here use an energy range extending at energies lower than the nominal recommended bandpass for illustration purposes.

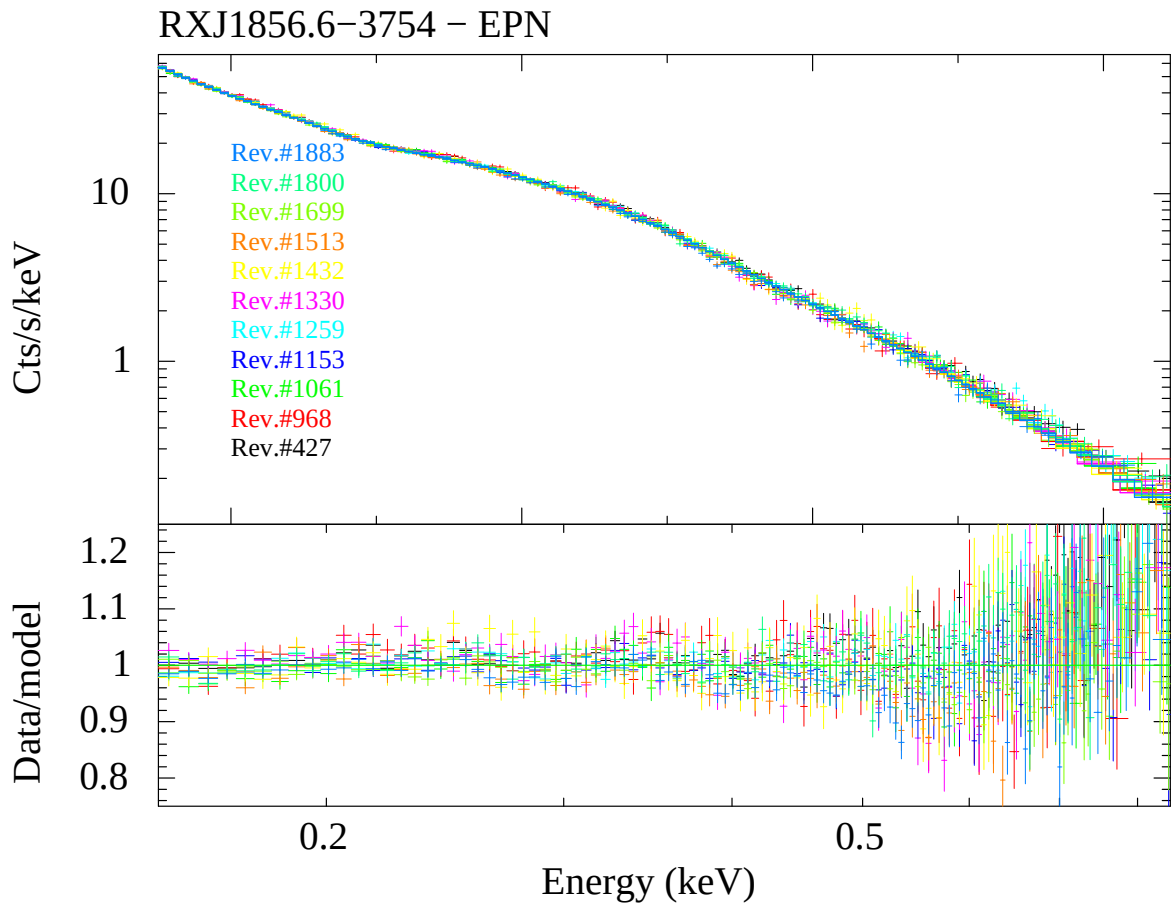

Figure 1: Spectra (*upper panel*) and residuals in units of data/model ratio (*lower panel*) for all the EPIC-pn observations of RXJ1856.6-3754 discussed in this document.

sure time (Obs.#041260010, $R(PHA)$) as reference. For each of the other spectra $S(PHA)$, we calculated the spectral shift ΔPHA which minimises the quantity: $\Sigma_i[S_i(PHA+\Delta PHA) - R_i(PHA)]^2/R_i(PHA)$. In Tab. 1 we report the ΔPHA values applied to each observation.

In Fig. 2 we show the distribution of the background-subtracted count rates in the PHA range between 40 and 200 (approximately corresponding to the nominal 0.2-0.8 keV energy band). The standard deviation of the distribution is 1.70% once normalized to its average (2.0% if no gain self-correction is applied). There is a marginal correlation between count rates and time (cf. Fig. 3; $R(t)=(5.584\pm0.011)-[(1.9\pm0.2)\times10^{-6}]t$). However, the scatter of the data points is dominated by a time-independent component. The relative energy-scale self-calibration removes any dependence of the count rate on the position of the source centroid in detector coordinates (Fig. 4).

On the other hand, the count rate during each of the observations is constant within statistics. We extracted source and background light curves from the same regions as background/source spectra with a binning time of 100 s. In Fig. 5 we show the distribution of the differences between the background subtracted count rates and their average during the observation, normalised to their statistical error of each measurement. The distributions are consistent with the statistical fluctuations.

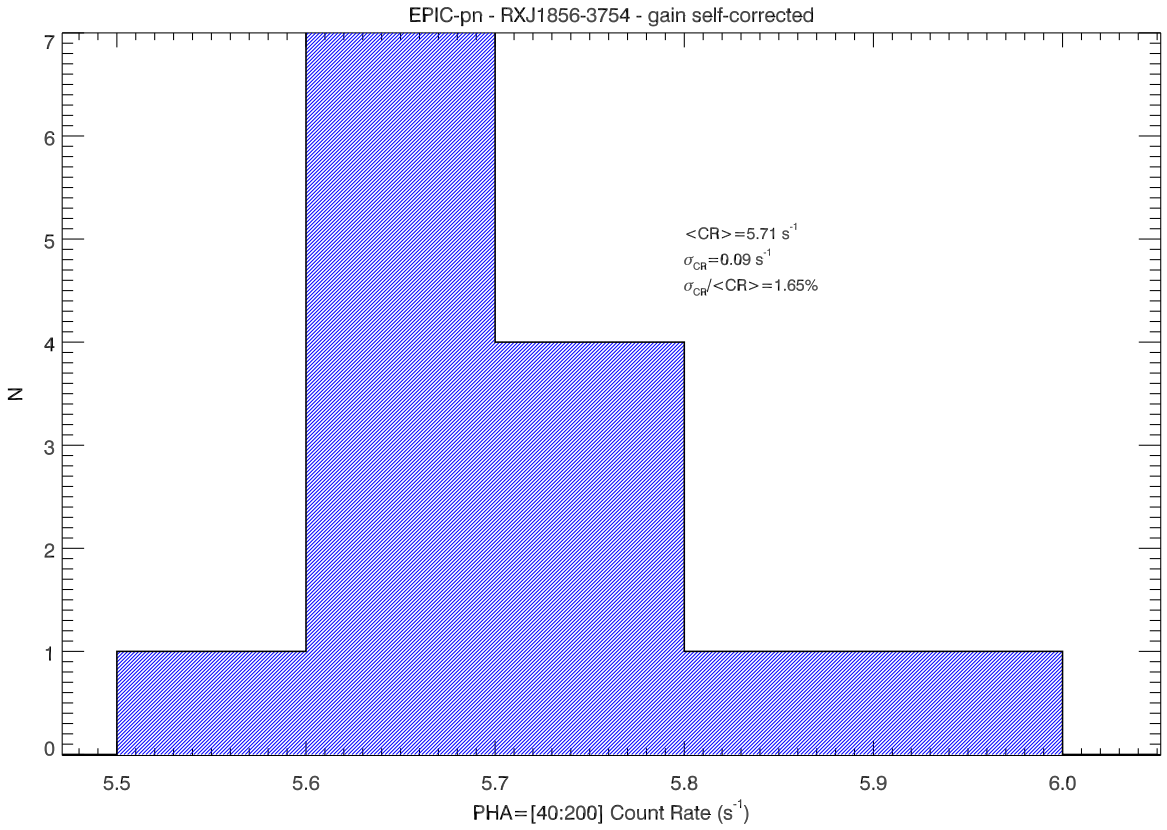

Figure 2: Distribution of the background-subtracted, time-averaged Count Rates (CR) in the 40–200 PHA range for all the on-axis EPIC-pn exposures of RXJ1856.6-3754 performed so far. The *inset* indicates the average, standard deviation, and standard deviation normalised to the mean of the distribution.

The energy-scale self-corrected EPIC-pn count rates are correlated with the normalisation of the simultaneous RGS exposures (Fig. 6). The correlation is mainly driven by the single data point with the largest count rate/normalisations. However, the data points are affected by a scatter larger than the statistical error bars. It is still unknown whether this scatter is due to instability of the EPIC-pn effective area or energy reconstruction, or to residual mis-calibration of the RGS contamination time evolution, or both.

5 Conclusions

We provide in this document a metric of the stability of the EPIC-pn camera, using the observations of the isolated neutron star RXJ1856.6-3754 performed so far (Tab. 1). We use the count rate in a PHA range nominally corresponding to the 0.2–0.8 keV energy range. After applying a relative self-calibration of the energy scale, to minimise any effect due to uncertainties in the column-by-column gain calibration, the normalised standard deviation of the count rate distribution is **1.70%** (Fig. 2). The scatter or the data points in the count rate versus time plane is dominated by a

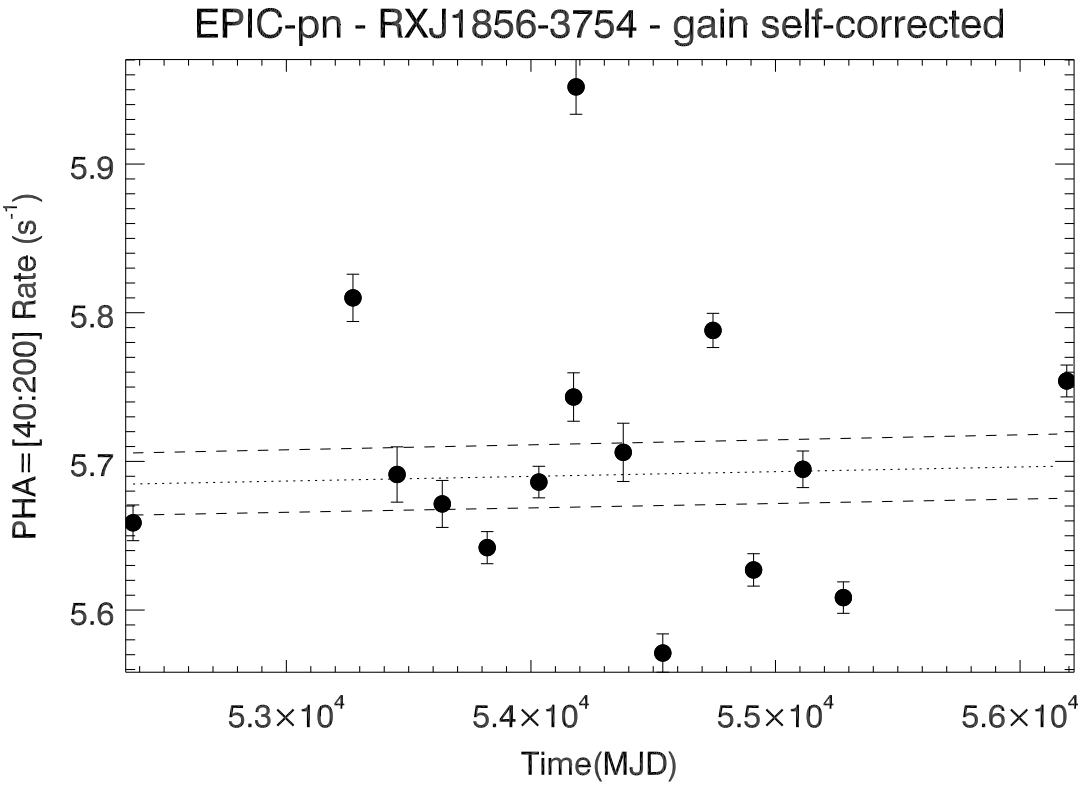

Figure 3: Background-subtracted, time-averaged CR in the 40–200 PHA range as a function of observation start time. The *dotted line* represent the best linear fit, the *dashed line* the envelope of the linear relation corresponding to a $\pm 1\sigma$ uncertainty on the best-fit parameters. The error bars indicate the Poissonian error calculated according to the Gehrels (1986) prescription.

time-independent component.

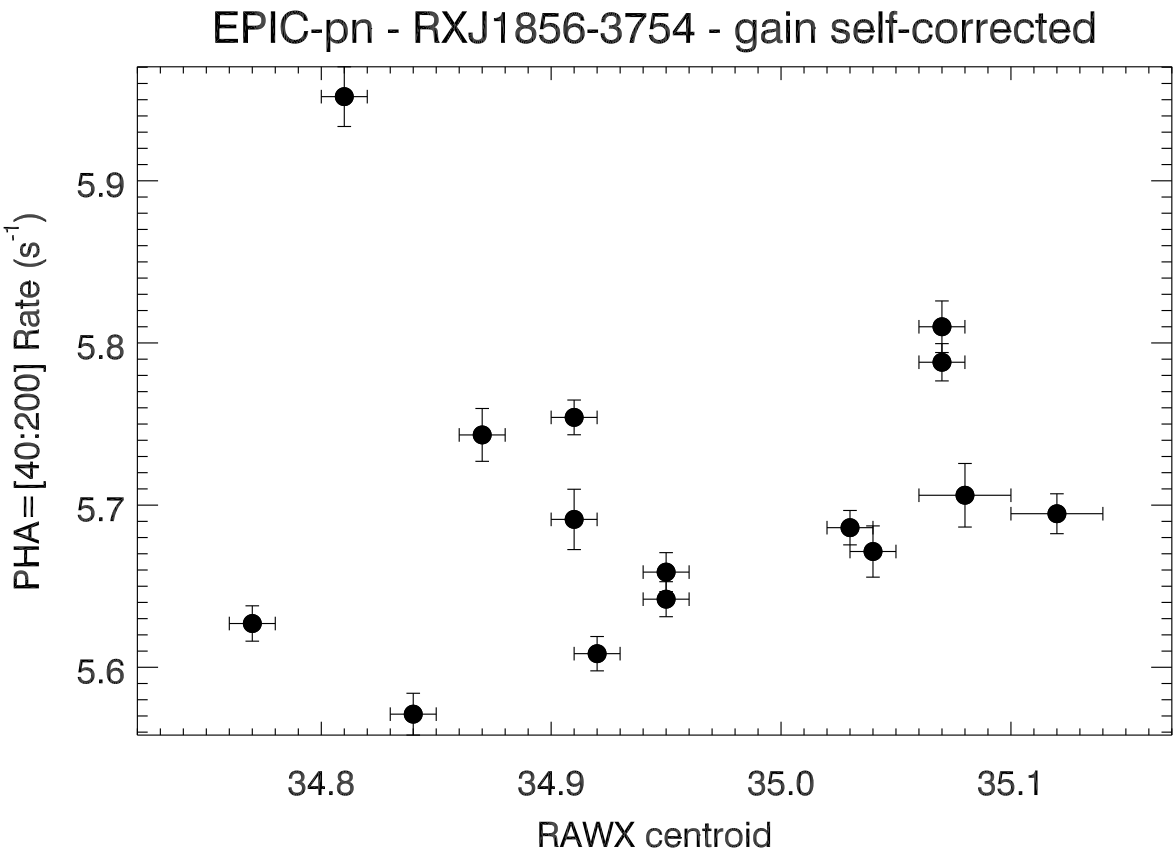

Figure 4: *Upper panel*: background-subtracted, time-averaged CR in the 40–200 PHA range as a function of the best-fit source centroid column (`RAWX`) for all the on-axis EPIC-pn exposures of RXJ1856.6-3754 performed so far.

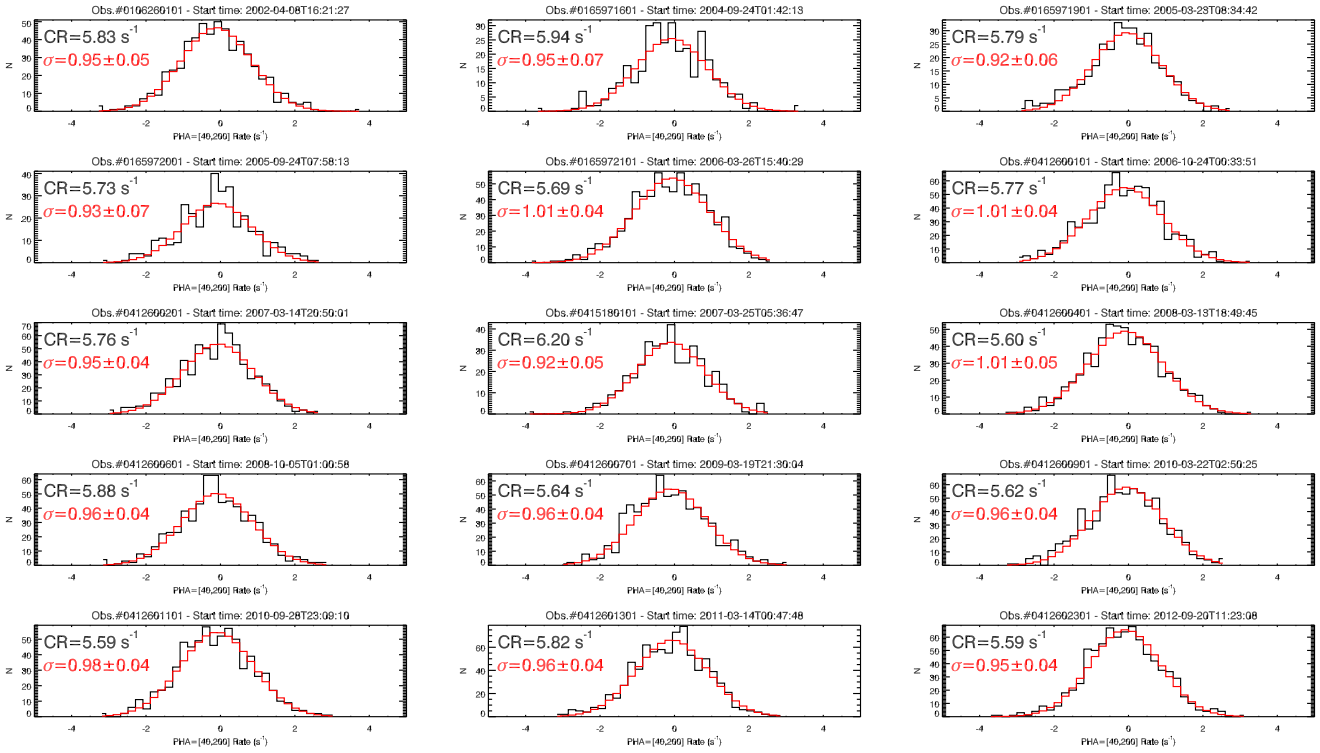

Figure 5: Distributions of the difference between the background subtracted count rates in the 40–200 PHA range in temporal bins of 100 seconds and their mean during the observation, normalised by the statistical error of each measurement (*black lines*). The red histogram is the fit of the observed distribution with a Gaussian function. In the *insets*: the average count rate, and the standard deviation of the fitted distribution.

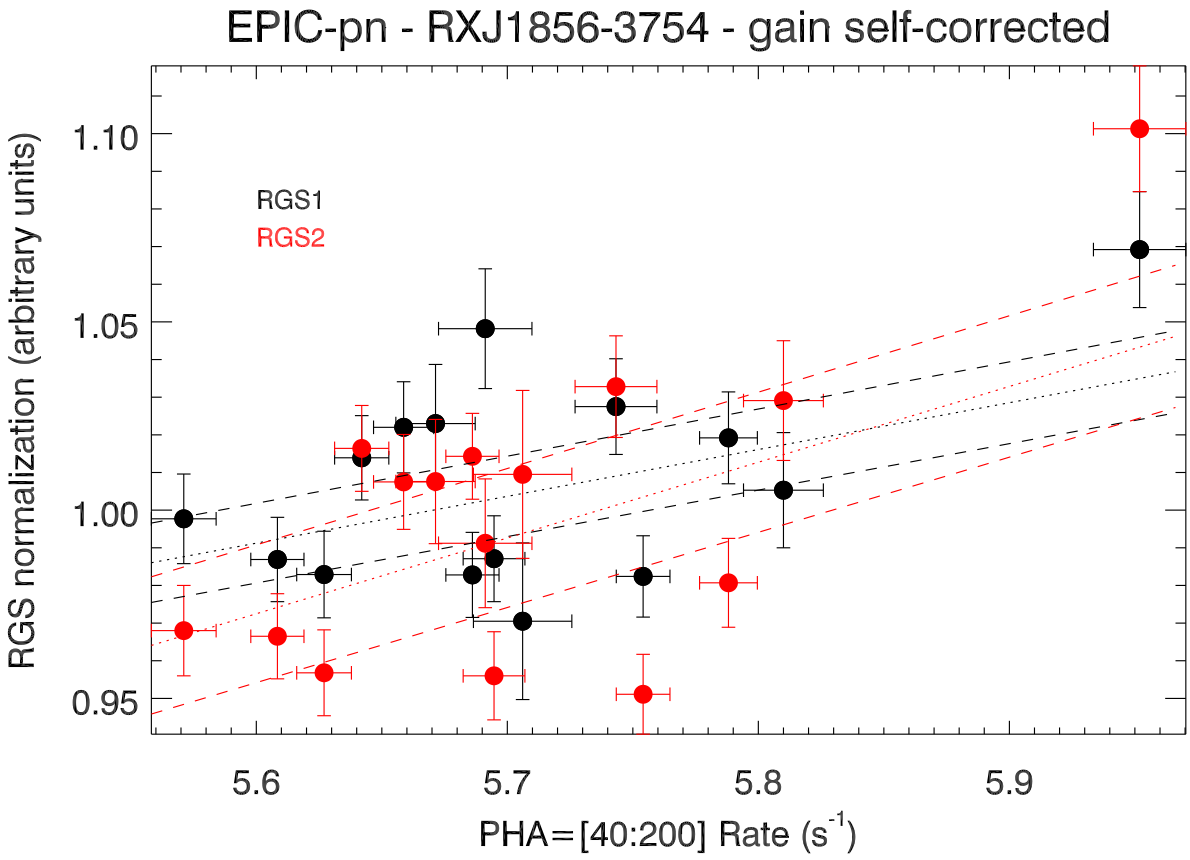

Figure 6: background-subtracted, time-averaged Count Rate (CR) in the 40–200 PHA range as a function of the blackbody spectral component normalisation (in relative units) in the simultaneous RGS exposures: *black*: RGS 1: *red*: RGS 2. The *dotted lines* indicate the linear best-fits; the *dashed lines* indicate the envelope corresponding to the $\pm 1\sigma$ uncertainties on the best-fit parameters.

References

Burwitz V. et al., 2001, A&A, 379, L35
Burwitz V. et al., 2001, A&A, 399, 1109
Gehrels N., 1986, ApJ, 303, 336
Guainazzi M. (Ed.), 2012, XMM-SOC-CAL-PL-0001[2]
Haberl F., et al., 2004, A&A, 419, 1077
Hambaryan V., et al., 2009, A&A, 497, L9
Ho W.C.G., et al., 2007, Ap&SS, 308, 279
Kaplan D.L. & van Kerkwijk M.H., 2005, ApJ, 628, L45
Sartore M., et al., 2012, A&A, 541, 66
Stuhlinger M., et al., 2011, XMM-SOC-CAL-TN-0052[3]
Strüder L., et al., 2001, A&A, 365, L18
Treves A., et al., 2000, PASP, 112, 297
Trümper J.E., 2004, NuPHS, 132, 560